

Technical Appendix

Metastability demystified — the foundational past, the pragmatic present, and the potential future

Authors

Fran Hancock^{1*}, Fernando E. Rosas^{2,3,4,5*}, Mengsen Zhang⁶, Pedro A. M. Mediano^{7,8}, Andrea I. Luppi⁹, Joana Cabral^{10,11}, Gustavo Deco^{12,13,14,15}, Morten L. Kringelbach^{5,10,16}, Michael Breakspear¹⁷, J.A. Scott Kelso^{18,19}, Federico E. Turkheimer¹

** These authors contributed equally to this work.*

E-mail: fran.hancock@kcl.ac.uk (FH), f.rosas@sussex.ac.uk (FR)

Table of contents

Preamble.....	3
Dynamical Systems Theory Primer.....	3
Phase space and manifolds	3
Stability in dynamical systems.....	4
Attractors, repellers, and saddles.....	5
Heteroclinic and homoclinic connections	6
Parameters in dynamical systems	7
Bifurcations	7
Phase transitions	9
Hallmarks of non-equilibrium phase transitions	9
Theoretical accounts of metastability.....	11
Background	11
Synergetics overview	11
Synergetics.....	11
Chaotic systems.....	12
Metastability without attractors or saddles – ghosts and ruins.....	12
Metastability with unstable attractors or saddles	13
Metastability with ghosts and homoclinic loops — Coordination Dynamics	14
Haken-Kelso-Bunz Model	15
Homoclinic loop.....	17
Metastability with unstable attractors — Chaotic itinerancy.....	17
Chaotic synchronisation.....	17
Stability of chaotic attractors.....	18
Metastability with saddles — Winnerless Competition	20
Kuramoto model	21
Derivation of metastability based on the variability of relative phase	23
Illustration of Phase Difference Differential	24
Implications of the generalised HKB model.....	27
References.....	29

Preamble

In the main manuscript we have provided an accessible account of metastability aimed at a general neuroscience audience. However, we expect that some readers with backgrounds in the physical sciences, engineering or mathematics would like to understand the theoretical aspects in more detail. This technical appendix was prepared to address these needs.

In this appendix we address different theoretical explanations for the dynamical phenomenon of metastability. These include bifurcation memory or ghosts in systems of coupled oscillators, homoclinic loops in systems exhibiting Sil'nov chaos, (attractor) ruins in chaotic systems exhibiting chaotic transience, Milnor attractors and riddled basins in chaotic systems exhibiting chaotic itinerancy, and finally, stable heteroclinic channels containing saddles in stochastic systems. In these systems metastability arises either with or without noise, and in some cases the addition of noise does not change the dynamics.

We reiterate some of the basics of dynamical systems theory for completeness which can easily be skipped over for the knowledgeable reader.

Dynamical Systems Theory Primer

Phase space and manifolds

Dynamical systems theory is a branch of mathematics that studies how the state of systems evolve over time based on either an analytical (pencil and paper), or a geometric (shapes), or a numeric (approximations using a computer) study of deterministic evolution equations. The *state* of a dynamical system is represented by a vector that fully determines the value of its variables (e.g., the position and velocity of a given particle). The temporal evolution of the state of a dynamical system can be mathematically described by a difference (i.e., discrete) or differential (i.e., continuous) equation.

The *phase space*¹ of a dynamical system is the set of all possible states, and hence contains all the allowed combinations of values of the system's variables (also known as *state variables*). A *trajectory* of the system is a sequence of states within the phase space that satisfy the dynamics of the system as defined by its differential equation.

A *phase portrait* is a geometric representation of the trajectories of a dynamical system. Some dynamical systems can also be illustrated as a *potential landscape* where valleys represent stable fixed points which correspond to attractors, peaks represent unstable fixed points which correspond to repellers, and balls represent the states of the system as in Figure 1 and 2.

A *manifold* is a geometric model that can represent a broad range of shapes. While at each point of a manifold it looks like a flat, n -dimensional (euclidian) space, their overall structure can be highly non-trivial. The dimensionality of the manifold, n , is the same for all its points.

Stability in dynamical systems

Equilibria or *fixed points* are points in the state space where the rate of change of the system with respect to time is equal to zero, corresponding to states at which the system remains unchanged unless perturbed. Fixed points can be *stable* or *unstable*, depending on whether neighbouring states move towards or away from them under the evolution rule (see Figure 1). A system is said to be *monostable* if just 1 stable fixed point exists, *bi-stable* if 2 exist, and *multistable* if 2 or more exist.

¹ For historical reasons, the term “phase” here does not refer to the phase of an oscillation, but more in general to the possible configurations that any system can explore (Nolte, 2010).

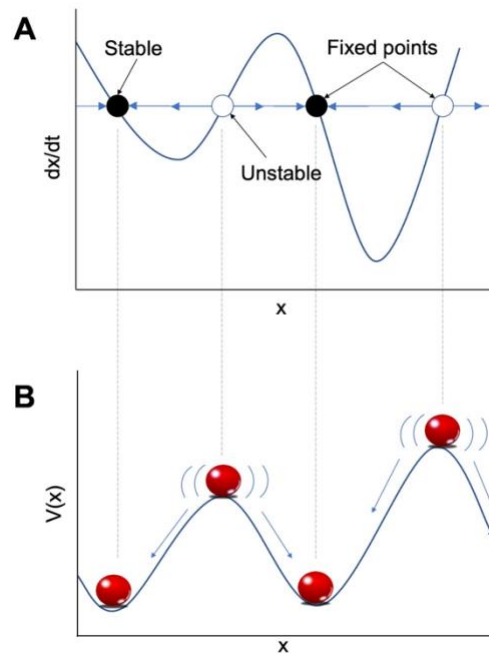


Figure 1. Phase portrait and potential landscape of a bistable dynamical system for a particular value of the control parameter. A) Phase portrait of a 1-dimensional dynamical system. The horizontal line presents a 1-dimensional state space (x). Horizontal blue arrows indicate the direction of the flow in the state space determined by the differential equation (dx/dt), which is plotted in black as a function of x . Where dx/dt is above (resp. below) the horizontal line, the trajectories in the state space flow to the right (resp. left) corresponding to a positive (resp. negative) change of the state variable. Where the function intersects with the horizontal level, there is no change to the state, making that value of x a fixed point. The slope of the function at the equilibrium point indicates its stability: a negative slope implies an attractor (i.e., a stable fixed point, as seen by nearby flows pointing towards the equilibrium), whilst a positive slope indicates a repeller (i.e., an unstable fixed point, as seen by nearby flows pointing away from the equilibrium). By convention, stable attracting points are represented by a filled circle, while repelling unstable points by an empty circle. **B)** Potential landscape of the same system. Valleys in this landscape represent stable fixed points, which may also be attractors. In contrast, peaks represent unstable fixed points which in this case are repellers.

Attractors, repellers, and saddles

Different initial conditions yield different trajectories. When many trajectories converge to a set of states, that set is called an *attractor*. Attractors may consist of a single point, a line, a periodic or quasi-periodic cycle, or can also have more complex geometries (usually called *strange* or *chaotic attractors*). A *chaotic attractor* is an attractor that holds dynamics that are highly sensitive to their initial conditions. The dynamics within a chaotic attractor are much harder to predict as they are neither at

equilibrium nor periodic. Each attractor is surrounded by its *basin of attraction* - all the points in phase space that flow onto the attractor. *Basin boundaries* separate basins of attraction. When many trajectories migrate away from a set of states, that set is called a *repeller*. When trajectories are attracted to a set of states in one direction but migrate away from the set in another direction, that set is called a *saddle*.

A *saddle* is a fixed point that is stable in one direction but unstable in another. It is dynamically unstable. The name comes from its representation in 2-dimensional systems (see Figure 2).

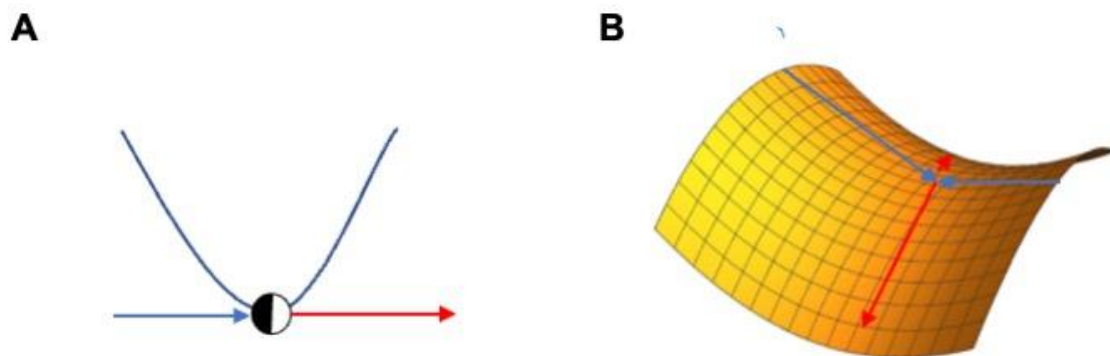


Figure 2 A saddle node in 1 and 2-dimensional systems. A) In a 1-dimensional system, the saddle is represented as a dual-coloured circle. The blue line shows the flow towards the saddle fixed point and the red line shows the flow away from the saddle. **B)** In a 2-dimensional system, it is easier to see how this fixed point got the name of a saddle node.

Heteroclinic and homoclinic connections

A *heteroclinic orbit or cycle* is a path in phase space that links saddles, and a *homoclinic cycle (or loop)* links a saddle back onto itself. See Figure 3.

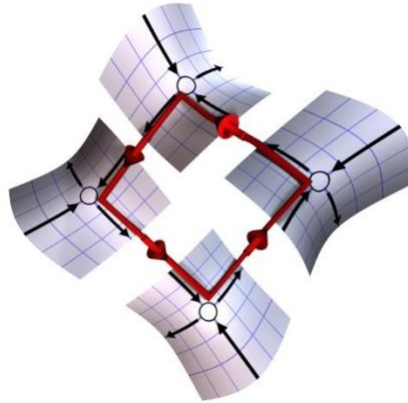


Figure 3. A heteroclinic cycle linking 4 saddles through their unstable directions. Reproduced with permission from Alexander Steele Kernbaum <https://www.researchgate.net/profile/Alexander-Kernbaum-2/research>.

Parameters in dynamical systems

Control parameters modify the system of differential or difference equations, hence deforming the corresponding flows through phase space. Quantitative changes in a *control parameter* can alter the qualitative structure of the resulting trajectories, which in turn can cause attractors (repellers) to be created, destroyed, or altered in their stability.

Destabilising an attractor fundamentally changes the shape of many trajectories. A qualitative change in the dynamical system is called a *bifurcation* (see BOX 4). The value of a control parameter at which a bifurcation occurs is known as a *critical point*. *Dynamic instabilities* refer to behavioural changes of the system in the vicinity of a bifurcation.

An *order parameter* is a single variable that captures the collective or macro behaviour of a system composed of microscopic elements.

Bifurcations

A *bifurcation* is a qualitative change in dynamics produced by varying a control parameter in a dynamical system. Importantly, there are different types of bifurcations depending on the dynamical properties of the system at each side of the bifurcation:

Pitchfork bifurcation – when one family of fixed points transfers its stability properties (stable or unstable) to two families in the vicinity of a critical point. If the stability properties transferred are stable, the bifurcation is *supercritical*. If the stability properties are unstable, the bifurcation is *subcritical*.

Saddle-node bifurcation – when a stable and an unstable fixed point collide and annihilate each other. In high-dimensional systems, a saddle-node bifurcation occurs when a saddle-node and fixed point collide.

Transcritical bifurcation – when two families of fixed points collide and exchange their stability.

Hopf bifurcation - when a stable fixed point transitions into a periodic ‘limit’ cycle attractor.

Bifurcation diagram - A bifurcation diagram follows how the landscape changes with the control parameter showing the location of attractors and repellers.

See Figure 4 for the associated *bifurcation diagrams*.

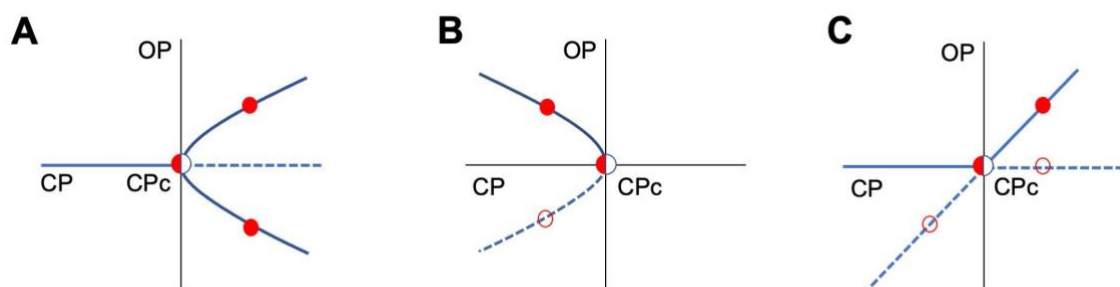


Figure 4. Bifurcation diagrams for different types of bifurcations. In these diagrams stable fixed points are shown with solid curves or lines and unstable fixed points with dotted curves or lines. A) A supercritical pitchfork bifurcation where a stable fixed point transfers its stability resulting in 2 new fixed points. The system may reside in either of the two states marked with red circles. B) A saddle-node bifurcation where a stable and unstable fixed point collide and annihilate each other. The saddle-node is stable in one direction and unstable in the other. C) A transcritical bifurcation where a stable and unstable fixed point collide and swap their stability. *Notation:* OP, order parameter; CP, control parameter; CPc, control parameter critical point.

Phase transitions

Phase transition – A concept originated from statistical physics. In general, a system is said to undergo a phase transition when a small change in a control parameter (e.g., temperature) causes a large collective change (e.g., the system going from liquid state to solid). A first-order or discontinuous phase transition is associated with a subcritical bifurcation, and a second order or continuous phase transition is associated with a supercritical bifurcation. Phase transitions refer to what is happening in the system and bifurcations reflect how it is happening.

Non-equilibrium phase transition – a phase transition that occurs in a physical system—like the brain—that is far from equilibrium. Such open systems ‘are kept in their active state by a continuous flux of energy into the system and by dissipation of energy’ [1,2]. Similar to equilibrium phase transitions, a small change in a control parameter (e.g., temperature from below) causes a large collective change (e.g. formation of convection rolls) as in the Rayleigh-Bénard instability [1,3]. The small change in the control parameter is sufficient to instigate the spontaneous formation of dynamic patterns in complex systems and are seen in a wide variety of disciplines. Physical examples include the laser (from incoherent to coherent light), hydrodynamic instabilities (formation of convection rolls when a liquid is heated from below), and the spiral patterns observed in certain chemical reactions. But there are many examples also in biology (e.g., predator-prey interactions, swarming patterns of fish and birds, termite architecture, etc.). Typical (predicted) phenomena associated with non-equilibrium phase transitions are revealed through the stochasticity in the system, which include *enhancement of fluctuations*, *critical slowing down* and *critical fluctuations*.

Hallmarks of non-equilibrium phase transitions

Enhancement of fluctuations. Fluctuations are sources of variability that exist in all dissipative systems. They kick the system away from the minimum and (on average) to a certain elevation in the potential landscape (Fig.1B). As a control parameter approaches a critical point, the magnitude of these *critical fluctuations* increases. This enhancement of fluctuations signals an upcoming phase transition.

Critical slowing down - Critical slowing down corresponds to the time it takes the system to recover from a small perturbation. Typically, if the system is far from a critical point, the effect of a small perturbation will decay quickly with time. *Relaxation time* is the time from the offset of the perturbation until the system returns to its previous steady state. However, as the system approaches a critical point, this decay will take longer and longer. That is, the relaxation time increases indicating a slowing down of the system and impending transition.

Multistable fluctuations – A system is stable if it resides either above or below a critical point, and weakly stable if it resides in the vicinity of a critical point. In a weakly stable system that undergoes a subcritical bifurcation, the stable solutions above and below the critical point co-exist and spontaneous switching between these attractors arises due to stochastic fluctuations in the system [4,5]. (See Figure 5).

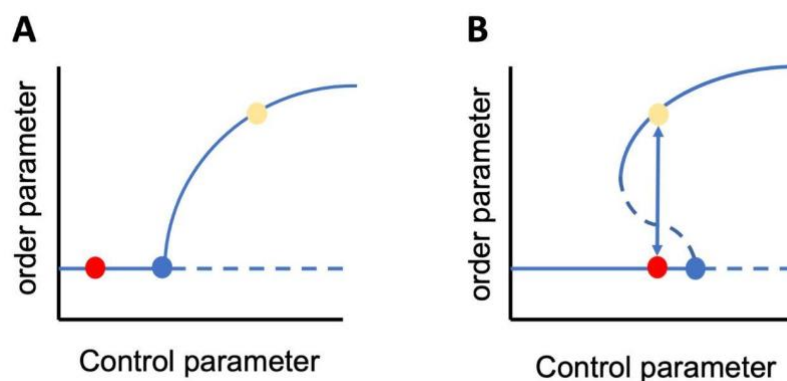


Figure 5. Multistable fluctuations. A) Stable solutions, the red and yellow points, away from the critical blue point, exist for different values of the order parameter. B) In the vicinity of the critical point, both stable solutions co-exist following a subcritical bifurcation. In the presence of noise or perturbations, the system spontaneously switches between the stable solutions. Adapted with permission from [6].

All these hallmarks of non-equilibrium phase transitions have been observed at both behavioural and brain levels [5,7 for a review,8]. In the context of synergetics (see Appendix A), such non-equilibrium phase transitions are indicative of a self-organising process [9–11].

Theoretical accounts of metastability

Inspired by the principles of synergetics and chaotic systems, the literature has proposed several different dynamical scenarios that can give rise to metastability. These scenarios can be classified as those with neither attractors nor saddles, those with unstable attractors, and those with saddles.

Background

Synergetics overview

Synergetics (from the Greek, “working together”) is a theory that aims at explaining how pattern formation takes place in self-organising systems composed of numerous weakly interacting elements that are thermodynamically open and far from equilibrium [12]. Synergetics focuses on scenarios where the interactions between the microscopic elements cause the system to organise into spatially and temporally ordered macroscopic patterns that can be described by a limited number of collective variables — known as *order parameters*. Such systems exhibit spontaneous pattern formation and switching, which occurs when one macroscopic pattern loses stability, and a new stable pattern takes its place. The contrast between the slow return of the macroscopic pattern and the fast dynamics of the underlying microscopic substrate generates a separation of timescales. Interestingly, during pattern formation the microscopic subsystems often adapt to the slow macroscopic dynamics, thus allowing macroscopic patterns (which are created bottom-up) to effectively ‘enslave’ its constituents ‘top-down’ — a concept known as the *slaving principle*. The bidirectional relationship between the macroscopic order parameters and the microscopic subsystems provides an operationalization of the notion of *circular* (or *reciprocal*) *causality*.

Synergetics

The rich spatiotemporal patterns that characterise the brain and other complex dynamical systems can be understood as being the result of nonlinear interactions and interdependencies that take place between their constituent elements [13–15].

Taking inspiration from statistical mechanics [16], one approach to study such collective self-organised behaviour is by identifying *order parameters* that effectively characterise different types of dynamics, while compressing the degrees of freedom of the complex systems [17]. Abrupt changes in order parameters (together with phenomena such as *critical fluctuations* and *critical slowing down*, see BOX 2) characterise transitions between different phases of the dynamics of the system, which are often triggered by changes in corresponding *control parameters* — which are variables often under the control of the researcher. Thus, the behaviour of order and control parameters allows for an efficient exploration of the possible dynamical behaviours of a complex system in terms of relatively simple signatures, which allows the researcher to identify different phases and understand how the system transitions between them. This approach is known as *Synergetics*.

Chaotic systems

Rich spatio-temporal patterns also arise in dynamical systems with chaotic attractors. A dynamical system is said to be chaotic when its behaviour is extremely sensitive to initial conditions (i.e., trajectories that initially start close together may end up very far apart), which makes long range forecasting of the system impossible. The complex evolutionary paths of such dynamical systems converge to chaotic or ‘strange’ attractors (see BOX 2). The most famous chaotic attractor is the Lorenz attractor which resembles two wings of a butterfly [18]. Despite this complexity, the system is described mathematically by just three evolutionary equations. Within neuroscience, biophysically plausible neural network models such as the Morris-Leclar model become chaotic when certain model parameters are set [19].

Metastability without attractors or saddles – ghosts and ruins

A first road to metastability concerns processes of bifurcation [20] [21–23]. Specifically, this road refers to scenarios where fixed points disappear after a bifurcation, but the “memory” of the fixed point remains attractive for the system and the dynamics become very slow [24] due to a bifurcation delay [25].

There is a well established literature that has developed these ideas. For example, in a Lorenz attractor, periodic fluctuations remain for a long time interval when a parameter (see BOX 8) is just above the critical value for transition to chaotic behaviour. This behaviour due to the memory or ghost for the periodic behaviour was classified as “Type I intermittency”, and has been illustrated with a Poincaré map² [26]. Also, the dynamical mechanism behind the phenomenon of saddle-node bifurcation memory was recently unveiled [27]. The phenomenon of fixed points that disappear but keep part of their attractive capabilities has also been described with the terms “ghost” [28–30], “phantom” [31], “almost attractor” [32], and “memory” [24], as the bifurcation delay gives the impression that the system remains attracted to the fixed point that disappears at the bifurcation.

A somehow related phenomenon is when a change in a control parameter makes a chaotic attractor undergo a boundary crisis bifurcation i.e., a collision with its own basin boundary [33]. Because of the collision, orbits on the attractor are now mapped onto another basin (and so onto another attractor) — the original attractor no longer exists and is referred to as a *ruin* [34]. Although the attractor no longer exists, a large set of initial conditions still approach the ruin transiently mimicking the behaviour of the former attractor before collapsing onto the alternative attractor, exhibiting *chaotic transience* [33–36]. The transient does not appear again unless the system’s parameters are reversed [34]. As metastability is characterised by patterns that *recur* either in repeatable sequences or flexible alternation, we therefore do not consider this type of transient behaviour as a valid example of metastability.

Metastability with unstable attractors or saddles

Another class of scenarios that can give rise to metastability are systems with so-called homoclinic and heteroclinic cycles connecting Milnor attractors (i.e., an attractor that is not asymptotically stable) or saddles. Homo- and heteroclinic cycles

² A Poincaré or first recurrence map, is the intersection of a periodic or chaotic orbit in the phase space of a continuous dynamical system with a certain lower-dimensional subspace, called the Poincaré section, transversal to the flow of the system.

are trajectories in phase space that connect unstable attractors or saddles through their unstable manifolds. That is the outset (repelled trajectories) of an unstable attractor or saddle are mapped to the inset (attracted trajectories) of itself (homo-) or another unstable attractor or saddle (hetero-). These cycles appear when the synchronisation of chaotic attractors is interrupted by bursts of desynchronisation [37–40], and in models of ‘winnerless competition’ (WLC) [41–45].

In the following we will restrict our detailed review to scenarios of 1) a ghost and a homoclinic loop in coordination dynamics, 2) heteroclinic cycles in chaotic itinerancy, and 3) stable heteroclinic channels in winnerless competition.

Metastability with ghosts and homoclinic loops — Coordination Dynamics

Metastability in coordination dynamics appears as relatively long periods of phase entrainment where phases are ‘*almost in sync*’, a behaviour called ‘*relative coordination*’, interrupted by rapid bursts of phase desynchronisation. The Synergetics framework was used to develop a mathematical model, the Haken-Kelso-Bunz [HKB: 46] which captured these, and other dynamics. At certain frequencies the model exhibited bi-stability (i.e., symmetric and antisymmetric rhythms), while only mono-stability (i.e., anti-symmetric) remained beyond a critical frequency [46]. Extensions to the original model showed that ‘*critical fluctuations*’ initiated the transition from symmetric to anti-symmetric rhythms at a critical frequency value [47]. A further extension, to take account of symmetry breaking when a metronome provided the rhythm frequency, discovered the metastable behaviour of epochs of relative coordination interspersed with loss of entrainment in the absence of noise. This behaviour was found when the control parameter, that is the frequency of the metronome, had a value just beyond the critical value which corresponded to a saddle-node bifurcation. Although the original fixed point no longer existed, trajectories remained attracted to where it once was exhibiting bifurcation memory or a ghost [48]. The original model and its extensions are described below, and the resulting dynamics are illustrated in Figure 6.

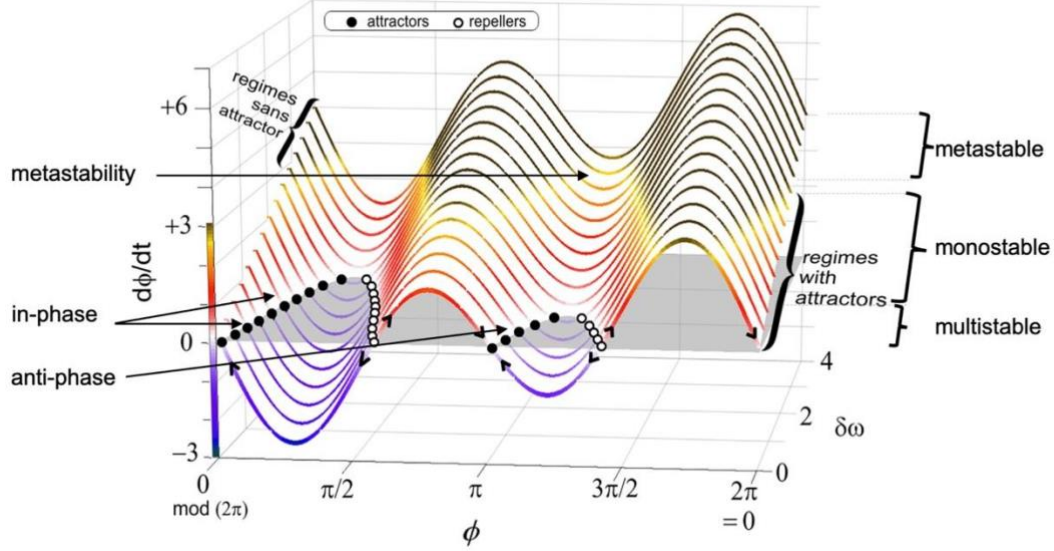


Figure 6. The rich dynamics in the HKB model illustrated in a phase portrait. A) The phase portrait of ϕ in the “extended” HKB model [48] for various values of a diversity (control) parameter $\delta\omega$. This graph carries regimes of coordination with attractors in the front of the figure (for modest diversity $\delta\omega$) and those without attractors (large diversity of the parts, shown in the back of the figure). Multi-, mono-, and metastable regimes are indicated to the right of the figure. Examples of anti-phase and in-phase attractors, and the absence of attractors in metastability, are shown on the left of the figure. Adapted with permission from [49].

Haken-Kelso-Bunz Model

The Haken-Kelso-Bunz model (HKB) [46], was developed to explain the coordinated dynamics of two oscillators with phases ϕ_1 and ϕ_2 — e.g., the movement trajectory of two fingers. The original model is given by the following dynamical equation:

$$\dot{\phi} = -a \sin\phi - 2b \sin 2\phi, \quad (\text{B1})$$

where $\phi = (\phi_2 - \phi_1)$ is the relative phase between the two oscillators, $\dot{\phi}$ is the derivative of ϕ with respect to time, and a and b describes the first-order and second-order coupling strength between the two oscillators.³ The order parameter is the

³ It was shown that the model could be derived from equations of motion of each hand and a nonlinear coupling between them based on coupled van der Pol-Rayleigh oscillators. The intrinsic

relative phase ϕ , and the control parameter is the coupling ratio b/a , which maps to the experimental manipulation of the movement frequency of the fingers. The HKB model was shown to reproduce experimental findings where, at a critical frequency, the system switched from having two attractors at 0 and π (both in-phase and anti-phase) to only one at 0 (in-phase) via a so-called pitchfork bifurcation (see Fig. 2A). More important for the theory-experiment relation was the identification of patterns of behaviour in terms of attractors, the existence of multistability (i.e., a dynamical system having multiple attractors) and the role of dynamic instability as a mechanism of change.

A next step was to extend the HKB model to include stochastic properties, which allowed it to demonstrate the decisive role of stochastic fluctuations in initiating the transition from anti-phase to in-phase [47]. The *stochastic HKB* model is given by

$$\dot{\phi} = -a \sin\phi - 2b \sin 2\phi + \sqrt{Q}\xi_t, \quad (\text{B2})$$

where ξ_t is a Gaussian white noise process⁴ and $Q > 0$ is the noise strength. An important assumption in Eq. (2) is that the frequencies of the two oscillators in the HKB model were the same. To empirically investigate what happens when this symmetry is broken, new experiments were performed where the movement of one finger was replaced with a metronome, and subjects were requested to synchronise peak flexion of the index finger with the metronome either off the beat or on the beat [48]. The resulting dynamic instability was observed to change dramatically [50–52]. To model this, the *extended stochastic HKB* model was introduced [48]:

$$\dot{\phi} = \delta\omega - a \sin\phi - b \sin 2\phi + \sqrt{Q}\xi_t \quad (\text{B3})$$

where the order parameter $\phi = (\phi_2 - \phi_1)$ is the phase, and $\delta\omega$ captures the difference in frequency between the metronome and the index finger movement.

dynamics of the hybrid Van der Pol-Rayleigh oscillators is defined by a linear self-excitation Van der Pol term and a Rayleigh saturation term.

⁴ A white noise process is a stochastic process satisfying the following conditions over its mean and autocorrelation: $\langle x_i \rangle = 0$, and $\langle x_i x_i' \rangle = \delta(x_i - x_i')$.

This model can be shown to contain a saddle node bifurcation [Figure 5. ; ,30]. Furthermore, just beyond the saddle in parameter space, the system remained attracted to where the stable and unstable fixed points once were — a phenomenon which became known as a *phantom attractor* [53] or an *attractor remnant* [30,52]. The system's behaviour in this régime was characterised as “metastable” [31].

Homoclinic loop

When the metronome experiment was repeated simultaneously with superconducting quantum interference device (SQUID) acquisition and the dominant spatial dynamics investigated [54], the signal dynamics observed in the brain closely resembled a model of Sil'nikov chaos [55], where the actual trajectories of the main spatial pattern displayed the geometry of homoclinic loops [56]. Independent of these studies, metastable states were shown to be linked by homo- and heteroclinic connections by analogy with physical systems [55] , and experimental and theoretical evidence was reported to support the hypothesis that phase transitions and metastability existed in the brain [57,58].

Metastability with unstable attractors — Chaotic itinerancy

In chaotic systems, metastability manifests as long periods of synchronisation between chaotic attractors interrupted by bursts of desynchronisation. This desynchronisation occurs when destabilised low-order unstable periodic orbits riddle the attractor basin with escape routes to other attractors. The chaotic attractor is now asymptotically unstable, and some trajectories leave in bursts of desynchronisation.

Chaotic synchronisation

When two chaotic dynamical systems attractors are uncoupled, their orbits follow chaotic trajectories that are asynchronous; however, if they are weakly coupled their orbits show stable synchronised motion [59,60]. To illustrate this idea, let's consider the behaviour of 3 state variables in a neural mass model: the mean membrane potential of local pyramidal cells V , the mean membrane potential of the inhibitory interneurons Z , and the average number of open potassium ion channels in a cortical

column W . Setting different values of the variance of the excitatory threshold dv , results in fixed point, limit cycle, or chaotic attractors. The chaotic regime arises specifically from the mixing of the fast timescales of the pyramidal cells and the slow responses of the inhibitory population [40]. When chaotic attractors synchronise, their orbits converge onto a smooth surface known as a *synchronisation manifold* whose shape is dependent on the type of synchronisation that occurs (see Figure 7).

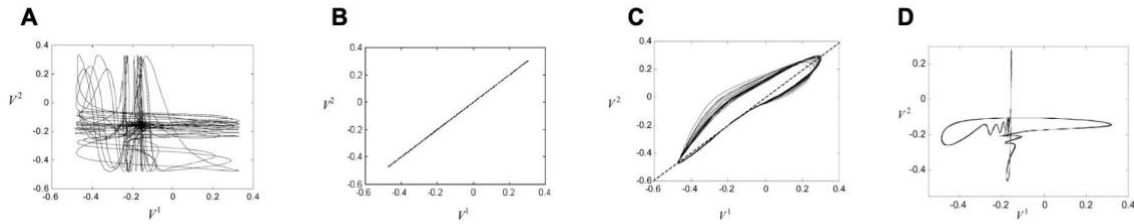


Figure 7. Chaotic synchronisation manifolds. Concurrent plots of average membrane potential of pyramidal neurons V^1 and V^2 in a neural mass model of cortical columns. **A)** If the potentials are uncoupled, their orbits follow chaotic trajectories that are asynchronous. **B)** If the potentials are weakly coupled, their orbits show stable synchronised motion, and the dynamics are governed by the same equations of motion as for a single chaotic attractor (Pecora & Carroll, 1990). **C)** If the 2 chaotic attractors are not identical, they will still synchronise, but the synchronisation manifold will be transformed [61]. **D)** Phase synchronisation manifold (extracted via the Hilbert transform) shows a highly structured chaotic phase synchronisation of two non-identical chaotic attractors [62]. Adapted and reproduced with permission from [40].

Stability of chaotic attractors

The stability of coupled chaotic attractors is typically contingent on the strength of their coupling. At a critical coupling value, transverse stability of the synchronisation manifold is lost, and the system undergoes a *blowout bifurcation* which transforms the attractor to a saddle as synchronisation is lost [63]. The chaotic system behaves differently on either side of this bifurcation [64]. In the vicinity above the bifurcation, a trajectory may spend a long time in the neighbourhood of the synchronisation manifold but occasionally burst out away from it to be reinjected close to the synchronisation manifold via a homoclinic orbit. In the absence of a reinjection mechanism, a trajectory may exhibit a super-persistent transient of chaotic motion before approaching some other attractor [64,65]. This behaviour is known as on-off

intermittency [66]. We do not consider on-off intermittency as a route to metastability as it fails to explain switching/cycling dynamics between two metastable states.

This system behaviour is related to riddled basins of attraction [64]. Chaotic attractors support a dense set of low-order (1 or 2-D) unstable periodic orbits or saddles [34,67]. These saddles are unstable tangential to the chaotic attractor and stable in the transverse direction [65]. See Figure 8 for a hypothetical example of an attracting periodic orbit illustrating 8a) tangential and transverse stability, and 8b) tangential stability and transverse instability.

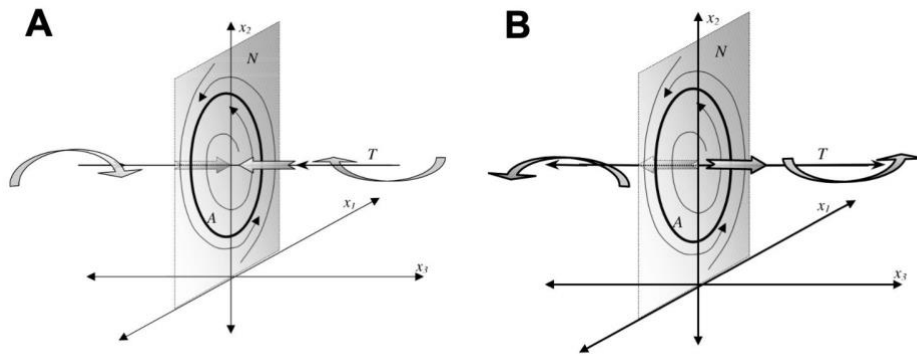


Figure 8. Phase space diagram illustrating transverse stability for hypothetical flow with periodic orbit A, embedded in the invariant manifold N. A is an attractor of the system confined to N, as illustrated by the thin arrows in the plane. **A)** A is also attracting in the transverse direction T, as illustrated by the ribbon arrows, and so is an asymptotically stable attractor in the full phase space. **B)** A is transversely unstable, and so is a saddle in the full phase space. Reproduced with permission from [38].

When a parameter changes (symmetry or membrane potential for example) such a saddle will also lose its transverse stability and repel orbits in the direction transverse to the chaotic attractor. This is called a *bubbling transition* [67] or *riddling bifurcation* [65]. The chaotic attractor is now weakly stable in the Milnor sense, that is it is no longer asymptotically stable, and its basin of attraction is riddled with points belonging to other attractors. Let us label one of these attractors as B, and the chaotic attractor A. A has become a *riddled basin attractor*. Additionally, in a

particular parameter range, nodes form clusters which partition the phase space into several basins of attraction [38,68]. In this case A and B represent different clusters. A number of initial conditions arbitrarily close to A, now with a riddled basin, will leave the neighbourhood of the synchronisation manifold to flow to attractor B [67]. If B is also a riddled basin attractor, the system may transition away from this attractor by the same mechanism, towards yet another riddled basin attractor C. The connections between A, B, and C are heteroclinic connections. If the cycle A-B-C repeats, the riddled basin Milnor attractors are contained within a “heteroclinic network” [69]. These riddled basin Milnor attractors are sometimes referred to as “quasi-attractors” and the neighbouring regions as “attractor ruins” [70] (not to be mistaken with a “ruin” following a boundary crisis in transient chaos). We consider the riddled basin Milnor attractors as metastable states, and *heteroclinic cycling* as a possible route to metastability with flexible alternation between metastable states, and *heteroclinic networks* as a possible route to metastability with repeatable transition sequences among metastable states.

Metastability with saddles — Winnerless Competition

The role of saddles in escaping from metastable states is well acknowledged in statistical physics [71]. Saddles play a central role in a mathematical model for metastability where metastable states are saddles linked through their unstable manifolds, where noise induces transitions through a heteroclinic sequence confined within a stable heteroclinic channel (SHC) [41,45,72]. SHC have been shown to be repeatable and robust to noise while remaining sensitive to informational input, and have been proposed to support cognitive and emotional processes [73]. The underlying model of neuronal activity is based on the winnerless competition principle [41]. Cognitive modes, consisting of specific collections of neuronal groups, are in constant competition for dominance, where each mode becomes the winner periodically. It has been proposed that sequential switching among saddles reflects this principle. Using a generalised Lotka-Volterra model which is the canonical model for Winnerless Competition (WLC) in the evolution of species, reproducible robust transient sequential activity within a SHC with 3 competing modes was demonstrated [45]. This model can be used to explain how such dynamics can be robust to noise

and reproducible, while the nature of the saddles ensures flexibility (see Figure 9). In such a picture, metastability may be seen as a delicate balance between robustness and flexibility. Although clusters are not considered specifically in SHCs, they have been demonstrated in stable heteroclinic cycles in a WLC model [74].

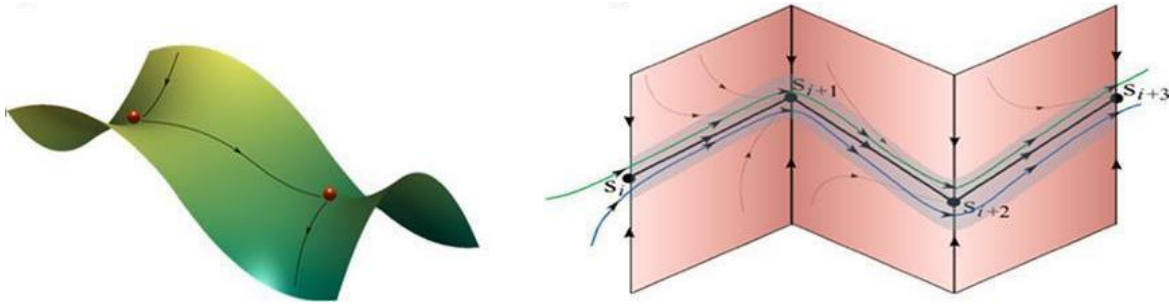


Figure 9. Representation of the ensemble of trajectories forming a heteroclinic channel. Left: a representation of a simple heteroclinic trajectory with two connected saddle nodes. **Right:** a representation of a stable heteroclinic channel – a robust sequence of saddle-nodes. Adapted with permission from [75].

Kuramoto model

The Kuramoto model of oscillators with sine coupling is given by

$$\dot{\phi} = \omega_k + \frac{\varepsilon}{N} \sum_{j=1}^N \sin(\phi_k - \phi_j), \quad (\text{A1})$$

where ϕ_k and ω_k is the phase and intrinsic frequency of the k th oscillator, ε is the amplitude of the force exerted by one oscillator on the other, N is the number of oscillators.

To derive the mean field, we rewrite x as

$$\dot{\phi} = \omega_k + \frac{\varepsilon}{N} \text{Im} \left(\sum_j \sin(\phi_k - \phi_j) \right), \quad (\text{A2})$$

Rearranging we get

$$\dot{\phi} = \omega_k + \varepsilon \text{Im} \left(e^{-i\phi_k} \frac{1}{N} \sum_j e^{i\phi_j} \right), \quad (\text{A3})$$

Where the mean field is

$$Y = \frac{1}{N} \sum_j e^{i\phi_j}, \quad (\text{A4})$$

Which is related to Ψ the phase, and R the amplitude of the collective mode,

$$\frac{1}{N} \sum_j e^{i\phi_j} = R e^{i\Psi}, \quad (\text{A5})$$

Phase synchronization is then defined as the modulo of the complex-valued order parameter.

$$PS = |R e^{i\Psi}| = \frac{1}{N} \left| \sum_j e^{i\phi_j} \right|, \quad (\text{A6})$$

The instantaneous phase synchrony is measured at each timepoint t is given by

$$iPS = |R e^{i\Psi(t)}| = \frac{1}{N} \left| \sum_j e^{i\phi_j(t)} \right| = |\langle e^{i\phi_j(t)} \rangle|, \quad (\text{A7})$$

And the variance of this instantaneous phase synchrony has been defined as a marker of metastability [e.g., 76].

$$\sigma_{met}(c) = \frac{1}{T-1} \sum_{t \leq T} (iPS_c(t) - \langle iPS_c \rangle_T)^2, \quad (\text{A8})$$

Derivation of metastability based on the variability of relative phase

Let R be the set of all N brain regions. Then for each time point t , the instantaneous phase-locking is calculated for all pairwise combinations of i and j , where $i, j \in R$

$$iPL_{ij} = \cos \left(\theta_i(t) - \theta_j(t) \right)_{i,j \in R}, \quad (\text{A9})$$

As the resulting matrix $iPL(t)$ is a symmetric, real valued matrix, the spectral theorem applies and thus, for each t , there exists an eigenbasis $\{v_i\}_{i=1}^N$ with associated eigenvalues $\{\lambda_i\}_{i=1}^N$:

$$iPL(t) = \sum_i \lambda_i v_i v_i' = \sum \lambda_i P_i = V \Lambda V' , \quad (\text{A10})$$

where the columns of V are the eigenvectors of iPL , Λ is the diagonal matrix of eigenvalues and P_i is the projector onto the subspace spanned by v_i . The leading eigenvector $V1(t)$ represents the main orientation of the phases over all brain regions at time t and partitions the N brain regions into two communities by separating the elements with different signs in $V1(t)$ [77]. The leading eigenvectors for all time points and for all subjects were concatenated into a $n \times p$ matrix $V1_{ALL}(t)$, where $n = (T_{max} * \text{number of subjects})$, T_{max} is the number of time points for each scan, and $p = N = \text{number of regions}$.

Five recurring spatiotemporal patterns or phase modes $\psi_{1,...,5}$ were derived from k-means clustering of the first or leading eigenvector $V1_{ALL}$. The centroids were ordered according to their average occurrence across all subjects. The first centroid ψ_1 , which occurred most frequently, represents a global mode where the instantaneous phase-locking in all regions was negative, that is all regions were in-

phase⁵. For any particular time t , the eigenvector $V1(t)$ has an arbitrary sign. Since $V1(t)$ and $-V1(t)$ represent the same vector orientation, the sign of $V1(t)$ was therefore flipped such that the most prevalent (dominant) sign was negative, in the following sense - if $\text{sum}(V1(t)) > 0$, $V1(t) = -V1(t)$. After clustering, regions from the cluster centroid with the non-dominant (positive) sign were selected. These regions were referred to as in antiphase⁶. The masks were then applied to $V1(t)$ resulting in five subsets $V1(t)_c$, $c \in \{1, \dots, 5\}$. Note that by definition $V1(t)_1$ is the complete set of all regions. Metastability was then calculated by computing the variance over time of each region in the five subsets $V1(t)_c$, $c \in \{1, \dots, 5\}$, and then taking the mean of these variances:

$$VAR_c = \langle \sigma_{V1_c} \rangle, \quad (A12)$$

Where

$$\sigma_{V1(c)} = \frac{1}{T-1} \sum_{t \leq T} (V1_{c(t)} - \langle V1_c \rangle_T)^2, \quad (A13)$$

Global VAR was then defined as the mean of VAR_c over all communities.

$$VAR_G = \langle VAR_c \rangle_c, \quad (A14)$$

Illustration of Phase Difference Differential

Figure 10 illustrates PDD in a bimodal phase-reduced Hansel-Moto-Meunier model consisting of the blue and burgundy oscillators. It is clear to see that the PDD tracks the frequency changes (Figure 310C of the oscillators, for example between 30 and 50 seconds. When the model includes all 5 oscillators, it is more difficult to interpret the PDDs (Figure 10D), but it is possible to plot the signature as the variance of the

⁵ Strictly speaking in-phase only occurs when the phase difference is 0 or an even multiplier of π . We use the term *in-phase* to refer to any out-of-phase relationship that amplifies the amplitude of the superimposed signals.

⁶ Strictly speaking antiphase only occurs when the phase difference is an odd multiplier of π . We use the term *antiphase* to refer to any out-of-phase relationship that attenuates the amplitude of the superimposed signals.

PDD, META_{PDD} (Figure 10E). Although the magnitudes are different, the order of META_{PDD} is similar to the order of META_{VAR} , calculated from Eqs. (A13) and (A14), as shown in Figure 10C.

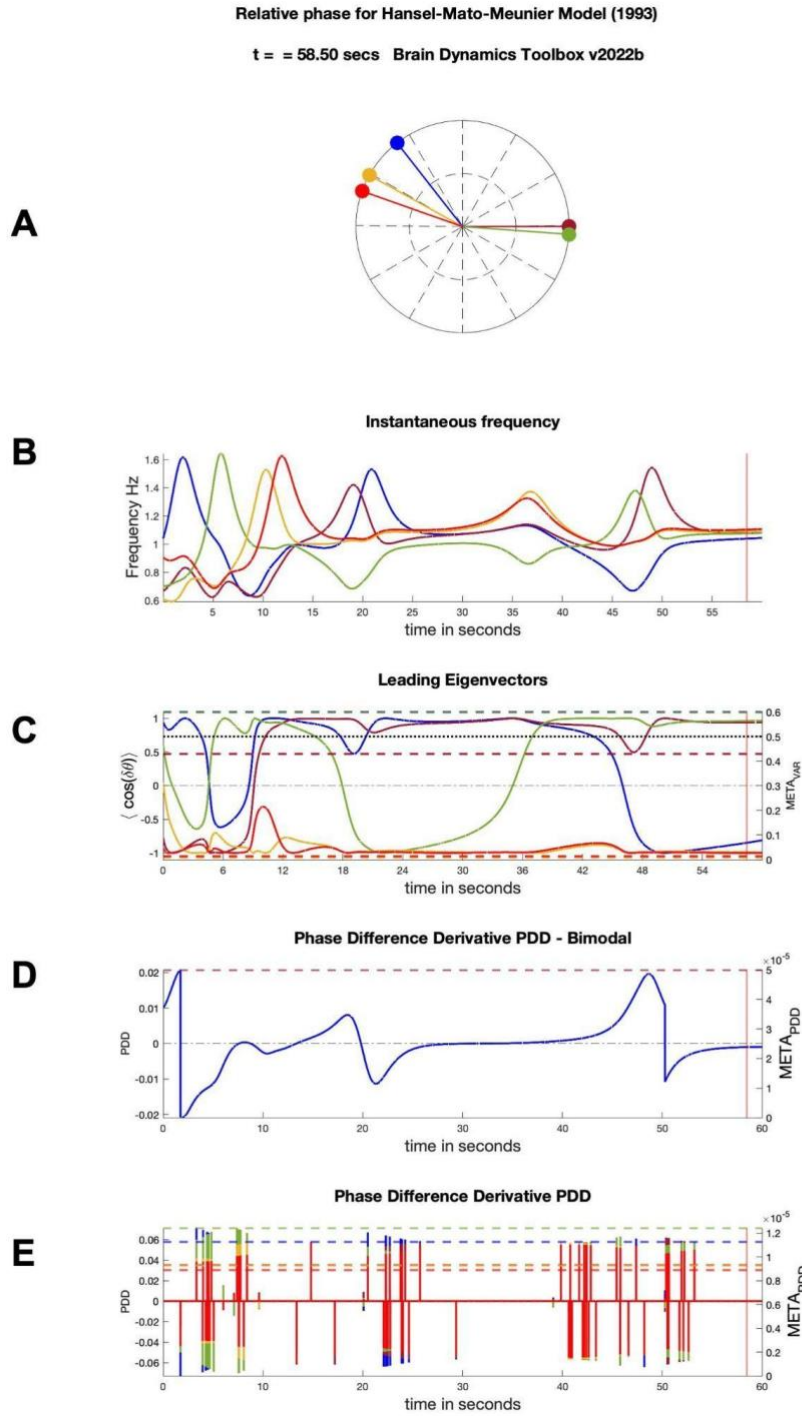


Figure 3. Phase Difference Derivative (PDD). Example from the Hansel-Moto-Meunier model of weakly excitatory, synaptically coupled Hodgkin–Huxley neurons [78]. **A)** Phases of individual neurons plotted on a unit circle. **B)** Instantaneous frequency of the individual neurons. **C)** Leading Eigenvectors for each individual neuron calculated analytically [79]. **D)** PDD between the neurons coloured blue and burgundy [80]. **E)** PDD between all neurons. Metastability measured as VAR plotted as dotted lines. Simulation created with the Brain Dynamics Toolbox v2022b [81]. $META_{PDD}$ metastability calculated as the variance of PDD. $META_{VAR}$ metastability calculated as the mean variance of the leading eigenvectors.

Implications of the generalised HKB model

Similar to the HKB model, the coupling ratio $\kappa = 2b/a$ controls the emergence of multistability at the critical value $\kappa_c=1$, beyond which any combinations of in-phase and antiphase coordination in the group become stable (given the oscillators are identical). Importantly, the critical value is invariant with respect to group size N , i.e., the onset of multistability is scale invariant. For $\kappa > \kappa_c$, the number of attractors grows exponentially (2^N) with group size for the generalised HKB model, while the canonical Kuromoto remains monostable.

The extensive multistability for high-dimensional HKB models paves the way for a complex form of spatiotemporal metastability – the more attractors there are in the multistable regime, the more ghosts there are in the metastable regime. Such high-dimensional metastable dynamics pose new challenges to theoretical and data analysis. First, due to the large number of ghosts, the repertoire of possible sequences of metastable dwells expands rapidly with system size – it becomes difficult to track each sequence individually and to analyse their robustness. While one can always resort to a statistical approach by studying the properties of the order parameter or order function, developing mathematical and data analysis tools suitable for characterising high-dimensional (microscopic) metastable sequences would be essential for understanding metastability as a general mechanism for sequence production (e.g., motor sequence generation, or episodic memory retrieval), where sequences that are functionally distinct at the microscopic level may become indistinguishable in their statistical dynamics. Second, this type of spatiotemporal metastability is multiscale in nature, while tailored analytical tools are scarce. As a reminder, in contrast to delay induced metastability in the above models, metastability in the extended HKB model and hence the generalised HKB model is induced by the symmetry breaking in the natural frequencies of the oscillators. Thus, metastability in the generalised HKB model implies the coexistence of multiple time scales, in terms of diversity in both the frequency of individual oscillators and dwell time between different pairs of oscillators. The metastability can also exist at different spatial scales, depending on the distribution of the oscillators'

natural frequencies and coupling strength (Figure 8). To capture the high-dimensional and multiscale features, tools from algebraic and computational topology have been introduced to the analysis of metastable dynamics [82,83]. A full-fledged mathematical theory is yet to be developed.

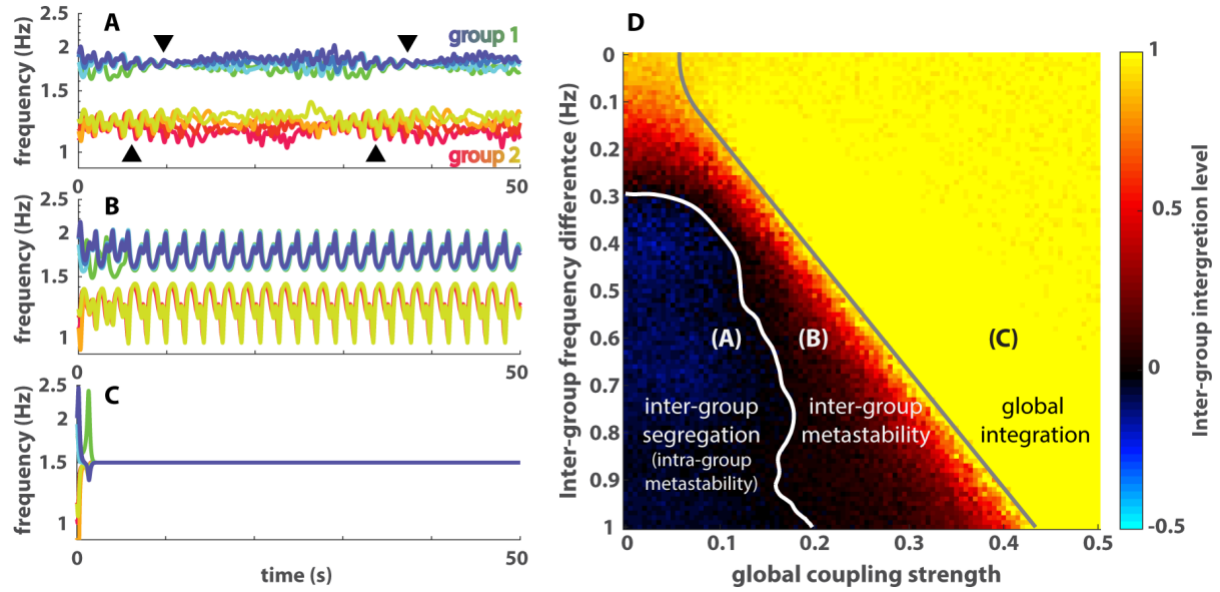


Figure 8. Metastability as multiscale phenomena in the generalised HKB model. (A-C) example dynamics of the generalised HKB model from 3 regimes in the parameter space (D) as the instantaneous frequency time series (i.e., time derivative of individual oscillator's phase). During metastable dwells, frequency trajectories approach each other; and during escapes, they diverge from each other. Dwells between different pairs of oscillators may occur together (black triangles in A). This particular implementation aims to capture the metastable dynamics observed in the “Human Firefly Experiment” [84], where participants were split into two frequency groups and the coordination dynamics was examined as a function of the intergroup frequency difference (experimentally manipulated). In (A-C), the intergroup frequency difference is 0.6 Hz, and coupling strengths were $a = b = 0.1, 0.2$, and 0.4 , respectively. In (A), weak coupling keeps the two groups segregated (refer to [85] for quantitative definition). However, members within the same group show metastable convergence and divergence (dwell and escape collectively). In (B), members within each group are phase-locked to each other, but members across groups engage each other in a metastable manner. In (C), all individuals are phase-locked together – metastability is lost. (The figure is adapted from Figure 4 of [85] with permission)

References

1. Haken H. Principles of Brain Functioning [Internet]. Heidelberg: Springer Berlin Heidelberg; 1995 [cited 2022 Oct 28]. 350 p. (Springer Series in Synergetics). Available from: <https://link.springer.com/book/10.1007/978-3-642-79570-1>
2. Prigogine I, Nicolis G. On Symmetry-Breaking Instabilities in Dissipative Systems. *J Chem Phys*. 1967;46(9):3542–50.
3. Kelso JAS. Dynamic patterns: The self-organization of brain and behavior. Cambridge, MA, US: The MIT Press; 1995. xvii, 334 p. (Dynamic patterns: The self-organization of brain and behavior).
4. Freyer F, Roberts JA, Becker R, Robinson PA, Ritter P, Breakspear M. Biophysical Mechanisms of Multistability in Resting-State Cortical Rhythms. *J Neurosci*. 2011 Apr 27;31(17):6353–61.
5. Schöner G, Kelso JAS. Dynamic Pattern Generation in Behavioral and Neural Systems. *Science*. 1988 Mar 25;239(4847):1513–20.
6. Cocchi L, Gollo LL, Zalesky A, Breakspear M. Criticality in the brain: A synthesis of neurobiology, models and cognition. *Prog Neurobiol*. 2017 Nov 1;158:132–52.
7. Kelso JAS. The Dynamic Brain in Action: Coordinative Structures, Criticality and Coordination Dynamics. In: Criticality in Neural Systems. Wiley-VCH Verlag GmbH & Co.; 2014. p. 67–104.
8. Kelso JAS, Bressler SL, Buchanan S, DeGuzman GC, Ding M, Fuchs A, et al. A phase transition in human brain and behavior. *Phys Lett A*. 1992 Sep 21;169(3):134–44.
9. Haken H. Synergetics. In: Yates FE, Garfinkel A, Walter DO, Yates GB, editors. Self-Organizing Systems [Internet]. Boston, MA: Springer US; 1987 [cited 2022 Nov 17]. p. 417–34. Available from: http://link.springer.com/10.1007/978-1-4613-0883-6_22
10. Kelso JAS. Phase Transitions: Foundations of Behavior. In: Haken H, Stadler M, editors. Synergetics of Cognition. Berlin, Heidelberg: Springer; 1990. p. 249–68. (Springer Series in Synergetics).
11. Kelso JAS. An Essay on Understanding the Mind. *Ecol Psychol Publ Int Soc Ecol Psychol*. 2008 Apr 1;20(2):180–208.
12. Haken H. Synopsis and Introduction. In: Basar E, editor. Synergetics of the brain: proceedings of the International Symposium on Synergetics at Schloss Elmau, Bavaria, May 2-7, 1983. Berlin ; New York: Springer-Verlag; 1983. (Springer series in synergetics).

13. Breakspear M, Terry JR. Nonlinear Interdependence in Neural Systems: Motivation, Theory, and Relevance. *Int J Neurosci*. 2002 Jan 1;112(10):1263–84.
14. Haken H. Cooperative phenomena in systems far from thermal equilibrium and in nonphysical systems. *Rev Mod Phys*. 1975 Jan 1;47(1):67–121.
15. Turkheimer FE, Rosas FE, Dipasquale O, Martins D, Fagerholm ED, Expert P, et al. A Complex Systems Perspective on Neuroimaging Studies of Behavior and Its Disorders. *The Neuroscientist*. 2021 Feb 16;1073858421994784.
16. Thurner S, Hanel R, Klimek P. *Introduction to the Theory of Complex Systems*. Oxford : New York: OUP Oxford; 2018. 448 p.
17. Haken H. Pattern Formation and Pattern Recognition — An Attempt at a Synthesis. In: Haken H, editor. *Pattern Formation by Dynamic Systems and Pattern Recognition*. Berlin: Springer; 1979.
18. Gleick J. *Chaos: making a new science*. New York, N.Y., U.S.A: Viking; 1987. 352 p.
19. Breakspear M. “Dynamic” connectivity in neural systems. *Neuroinformatics*. 2004 Jun 1;2(2):205–24.
20. Feigin MI, Kagan MA. Emergencies as a manifestation of the effect of bifurcation memory in controlled unstable systems. *Int J Bifurc Chaos*. 2004 Jul;14(07):2439–47.
21. Neishtadt A. Prolongation of the loss of stability in the case of dynamic bifurcations. II. *Differ Equ*. 1988;24(2):171–6.
22. Neishtadt A. On stability loss delay for dynamical bifurcations. *Am Inst Math Sci [Internet]*. 2009 [cited 2023 Jun 1];2(4). Available from: <https://www.aims sciences.org/article/doi/10.3934/dcdss.2009.2.897>
23. Neishtadt AI, Simó C, Treschev DV. On stability loss delay for a periodic trajectory. In: Broer HW, van Gils SA, Hoveijn I, Takens F, editors. *Nonlinear Dynamical Systems and Chaos*. Basel: Birkhäuser; 1996. p. 253–78. (Progress in Nonlinear Differential Equations and Their Applications).
24. Breakspear M, Jirsa V. *Handbook Of Brain Connectivity [Internet]*. Berlin Heidelberg: Springer; 2007 [cited 2023 Jun 2]. Available from: <https://vdoc.pub/documents/handbook-of-brain-connectivity-1shrf0dto5lg>
25. Kuehn C. Scaling of saddle-node bifurcations: degeneracies and rapid quantitative changes. *J Phys Math Theor*. 2008 Dec;42(4):045101.
26. Pomeau Y, Manneville P. Intermittent transition to turbulence in dissipative dynamical systems. *Commun Math Phys*. 1980 Jun 1;74(2):189–97.

27. Canela J, Alsedà L, Fagella N, Sardanyés J. Dynamical mechanism behind ghosts unveiled in a map complexification. *Chaos Solitons Fractals*. 2022 Mar 1;156:111780.
28. Izhikevich EM. *Dynamical systems in neuroscience: the geometry of excitability and bursting*. Cambridge, Mass: MIT Press; 2007. 441 p. (Computational neuroscience).
29. Kelso JAS, DeGuzman GC, Holroyd T. Synergetic Dynamics of Biological Coordination with Special Reference to Phase Attraction and Intermittency. In: Haken H, Koepchen HP, editors. *Rhythms in Physiological Systems*. Berlin, Heidelberg: Springer; 1991. p. 195–213. (Springer Series in Synergetics).
30. Strogatz SH. *Nonlinear dynamics and chaos: with applications to physics, biology, chemistry, and engineering*. 2nd Edition. Boca Raton: CRC Press; 2015. 532 p.
31. Kelso JAS. Coordination Dynamics of Human Brain and Behavior. In: Friedrich R, Wunderlin A, editors. *Evolution of Dynamical Structures in Complex Systems*. Berlin, Heidelberg: Springer; 1992. p. 223–34. (Springer Proceedings in Physics).
32. Eckmann JP, Ruelle D. Ergodic theory of chaos and strange attractors. *Rev Mod Phys*. 1985 Jul 1;57(3):617–56.
33. Grebogi C, Ott E, Yorke JA. Crises, sudden changes in chaotic attractors, and transient chaos. *Phys Nonlinear Phenom*. 1983 May 1;7(1):181–200.
34. Breakspear M, Friston K. Symmetries and itineracy in nonlinear systems with many degrees of freedom. *Behav Brain Sci*. 2001 Oct;24(5):813–813.
35. Friston KJ. The Labile Brain. II. Transients, Complexity and Selection. *Philos Trans Biol Sci*. 2000;355(1394):237–52.
36. Ott E. *Chaos in Dynamical Systems* [Internet]. 2nd ed. Cambridge: Cambridge University Press; 2002 [cited 2022 Nov 30]. Available from: <https://www.cambridge.org/core/books/chaos-in-dynamical-systems/7A0749AE3FBBF4312A54D7573C2DAAB5>
37. Ashwin P, Burylko O, Maistrenko Y. Bifurcation to heteroclinic cycles and sensitivity in three and four coupled phase oscillators. *Phys Nonlinear Phenom*. 2008 Apr 1;237(4):454–66.
38. Breakspear M. Perception of odors by a nonlinear model of the olfactory bulb. *Int J Neural Syst*. 2001 Apr;11(2):101–24.
39. Breakspear M. Nonlinear phase desynchronization in human electroencephalographic data. *Hum Brain Mapp*. 2002;15(3):175–98.
40. Breakspear M, Terry JR, Friston KJ. Modulation of excitatory synaptic coupling facilitates synchronization and complex dynamics in a biophysical model of neuronal dynamics. *Netw Comput Neural Syst*. 2003 Jan;14(4):703–32.

41. Afraimovich V, Rabinovich M, Varona P. Heteroclinic Contours in Neural Ensembles and the Winnerless Competition Principle. *Int J Bifurc Chaos*. 2003 May 10;14.
42. Ashwin P, Lavric A. A low-dimensional model of binocular rivalry using winnerless competition. *Phys Nonlinear Phenom*. 2010 May 1;239(9):529–36.
43. beim Graben P, Jimenez-Marin A, Diez I, Cortes JM, Desroches M, Rodrigues S. Metastable Resting State Brain Dynamics. *Front Comput Neurosci* [Internet]. 2019 [cited 2020 Nov 17];13. Available from: <https://www.frontiersin.org/articles/10.3389/fncom.2019.00062/full>
44. Hutt A, beim Graben P. Sequences by Metastable Attractors: Interweaving Dynamical Systems and Experimental Data. *Front Appl Math Stat* [Internet]. 2017 [cited 2023 May 28];3. Available from: <https://www.frontiersin.org/articles/10.3389/fams.2017.00011>
45. Rabinovich MI, Huerta R, Varona P, Afraimovich VS. Transient Cognitive Dynamics, Metastability, and Decision Making. *PLOS Comput Biol*. 2008 May 2;4(5):e1000072.
46. Haken H, Kelso JAS, Bunz H. A theoretical model of phase transitions in human hand movements. *Biol Cybern*. 1985 Feb 1;51(5):347–56.
47. Schöner G, Haken H, Kelso JAS. A stochastic theory of phase transitions in human hand movement. *Biol Cybern*. 1986 Feb 1;53(4):247–57.
48. Kelso JAS, Del Colle JD, Schöner G. Action-perception as a pattern formation process. In: *Attention and performance 13: Motor representation and control*. Hillsdale, NJ, US: Lawrence Erlbaum Associates, Inc; 1990. p. 139–69.
49. Tognoli E, Zhang M, Fuchs A, Beetle C, Kelso JAS. Coordination Dynamics: A Foundation for Understanding Social Behavior. *Front Hum Neurosci*. 2020;14:317.
50. Fuchs A, Jirsa VK, Haken H, Kelso JAS. Extending the HKB model of coordinated movement to oscillators with different eigenfrequencies. *Biol Cybern*. 1996 Jan 1;74(1):21–30.
51. Fuchs A, Kelso JAS. A Theoretical Note on Models of Interlimb Coordination. *J Exp Psychol Hum Percept Perform*. 1994 Nov 1;20:1088–97.
52. Kelso JAS, Jeka JJ. Symmetry breaking dynamics of human multilimb coordination. *J Exp Psychol Hum Percept Perform*. 1992;18:645–68.
53. DeGunzman, Kelso JAS. The Flexible Dynamics of Biological Coordination: Living in the Niche between Order and Disorder. In: Mittlethal JE, editor. *Principles Of Organization In Organisms*. Addison-Wesley; 1992.
54. Fuchs A, Kelso JAS, Haken H. Phase transitions in the human brain: spatial mode dynamics. *Int J Bifurc Chaos*. 1992 Dec 1;02(04):917–39.

55. Couillet P, Tresser C, Arnéodo A. Transition to stochasticity for a class of forced oscillators. *Phys Lett A*. 1979 Jul 23;72(4):268–70.
56. Kelso JAS, Fuchs A. Self-organizing dynamics of the human brain: Critical instabilities and Sil'nikov chaos. *Chaos Woodbury N*. 1995 Mar;5(1):64–9.
57. Holden AV, Kryukov VI. *Neural Networks: theory and architecture*. Manchester University Press; 1990.
58. Kryukov V. The metastable and unstable states in the brain. *Neural Netw*. 1988 Dec 31;1:264.
59. Fujisaka H, Yamada T. A New Intermittency in Coupled Dynamical Systems. *Prog Theor Phys*. 1985 Oct 1;74:918–21.
60. Pecora LM, Carroll TL. Synchronization in chaotic systems. *Phys Rev Lett*. 1990 Feb 19;64(8):821–4.
61. Afraimovich V, Verichev NN, Rabinovich MI. Stochastic synchronization of oscillation in dissipative systems. *Radiophys Quantum Electron*. 1986 Sep 1;29:795–803.
62. Rosenblum MG, Pikovsky AS, Kurths J. Phase Synchronization of Chaotic Oscillators. *Phys Rev Lett*. 1996 Mar 11;76(11):1804–7.
63. Ott E, Sommerer JC. Blowout bifurcations: the occurrence of riddled basins and on-off intermittency. *Phys Lett A*. 1994 May 9;188(1):39–47.
64. Maistrenko YuL, Maistrenko VL, Popovich A, Mosekilde E. Transverse instability and riddled basins in a system of two coupled logistic maps. *Phys Rev E*. 1998 Mar 1;57(3):2713–24.
65. Lai YC, Grebogi C, Yorke JA, Venkataramani SC. Riddling Bifurcation in Chaotic Dynamical Systems. *Phys Rev Lett*. 1996 Jul 1;77(1):55–8.
66. Platt N, Spiegel EA, Tresser C. On-off intermittency: A mechanism for bursting. *Phys Rev Lett*. 1993 Jan 18;70(3):279–82.
67. Ashwin P, Buescu J, Stewart I. Bubbling of attractors and synchronisation of chaotic oscillators. *Phys Lett A*. 1994 Sep 26;193(2):126–39.
68. Kaneko K. Clustering, coding, switching, hierarchical ordering, and control in a network of chaotic elements. *Phys Nonlinear Phenom*. 1990 Mar 1;41(2):137–72.
69. Ashwin P, Postlethwaite C. On designing heteroclinic networks from graphs. *Phys Nonlinear Phenom*. 2013 Dec 15;265:26–39.
70. Tsuda I. Toward an interpretation of dynamic neural activity in terms of chaotic dynamical systems. *Behav Brain Sci*. 2001 Oct;24(5):793–810.

71. Hanggi P. Escape from a metastable state. *J Stat Phys*. 1986 Jan 1;42(1):105–48.
72. Afraimovich V, Zhigulin VP, Rabinovich MI. On the origin of reproducible sequential activity in neural circuits. *Chaos Woodbury N*. 2004 Dec;14(4):1123–9.
73. Afraimovich V, Muezzinoglu MK, Rabinovich MI. Metastability and Transients in Brain Dynamics: Problems and Rigorous Results. In: Luo ACJ, Afraimovich V, editors. *Long-range Interactions, Stochasticity and Fractional Dynamics: Dedicated to George M Zaslavsky (1935–2008)* [Internet]. Berlin, Heidelberg: Springer; 2010 [cited 2023 May 26]. p. 133–75. (Nonlinear Physical Science). Available from: https://doi.org/10.1007/978-3-642-12343-6_4
74. Ashwin P, Karabacak Ö, Nowotny T. Criteria for robustness of heteroclinic cycles in neural microcircuits. *J Math Neurosci*. 2011 Nov 28;1(1):13.
75. Rabinovich MI, Varona P. Robust Transient Dynamics and Brain Functions. *Front Comput Neurosci*. 2011 Jun 13;5:24.
76. Shanahan M. Metastable chimera states in community-structured oscillator networks. *Chaos Interdiscip J Nonlinear Sci*. 2010 Mar;20(1):013108.
77. Newman MEJ. Finding community structure in networks using the eigenvectors of matrices. *Phys Rev E*. 2006 Sep 11;74(3):036104.
78. Hansel D, Mato G, Meunier C. Clustering and slow switching in globally coupled phase oscillators. *Phys Rev E*. 1993 Nov 1;48(5):3470–7.
79. Alteriis G de, MacNicol E, Hancock F, Cash D, Expert P, Turkheimer FE. EiDA: A Lossless Approach for the Dynamic Analysis of Connectivity Patterns in Signals; Application to Resting State fMRI of a Model of Ageing [Internet]. *bioRxiv*; 2023 [cited 2023 Mar 31]. p. 2023.02.27.529688. Available from: <https://www.biorxiv.org/content/10.1101/2023.02.27.529688v1>
80. Breakspear M, Williams LM, Stam CJ. A Novel Method for the Topographic Analysis of Neural Activity Reveals Formation and Dissolution of ‘Dynamic Cell Assemblies’. *J Comput Neurosci*. 2004 Jan 1;16(1):49–68.
81. Heitmann S, Aburn MJ, Breakspear M. The Brain Dynamics Toolbox for Matlab. *Neurocomputing*. 2018 Nov 13;315:82–8.
82. Mengsen Zhang. *The Coordination Dynamics of Multiple Agents*. 2018.
83. Zhang M, Kalies WD, Kelso JAS, Tognoli E. Topological portraits of multiscale coordination dynamics. *J Neurosci Methods*. 2020;108672.
84. Zhang M, Kelso JAS, Tognoli E. Critical diversity: Divided or united states of social coordination. *PLOS ONE*. 2018 Apr 4;13(4):e0193843.

85. Zhang M, Beetle C, Kelso JAS, Tognoli E. Connecting empirical phenomena and theoretical models of biological coordination across scales. *J R Soc Interface*. 2019 Aug;16(157):20190360.